SUPPLEMENTAL METHODS

Histology

For histological and immunohistochemical analysis, ear sections were harvested after depilation, briefly fixed in 4% ice cold paraformaldehyde (Sigma-Aldrich), and paraffin-embedded. Hematoxylin and eosin sections were prepared using standard techniques and subcutaneous tissue thickness analysis was performed by two blinded reviewers (n = 6 per group).

Immunohistochemical staining was performed according to our established techniques (Avraham *et al.*, 2010). After antigen retrieval, tissues were incubated with primary antibody overnight at 4°C and antibody staining was visualized using horseradish-peroxidase-conjugated secondary antibodies developed with diaminobenzamine complex (DAB; Vector, Burlingame, CA). Primary antibodies used for immunohistochemical stains included LYVE-1, CD45, and CCL21 (all from R&D, Minneapolis, MN), iNOS and CD11b (both from BD biosciences, San Jose, CA), CD3 (Dako North America, Inc. Carpinteria, CA), podoplanin, F4/80, and VEGFR-3 (all from Abcam, Cambridge, MA), CD31 (EMD Millipore, Billerica, MA) and perilipin (Fitzgerald Industries International, Acton, MA). All secondary antibodies were obtained from Vector Laboratories (Burlingame, CA) and eBioscience (San Diego, CA). Sections were scanned using a Mirax slide scanner (Carl Zeiss, Jena, Germany) and analyzed using Pannoramic Viewer (3D HISTECH, Budapest, Hungary). Cell counts were performed on high-power sections, with a minimum of 4–6 animals per group and 4–5 high power fields (HPF)/animal by two blinded reviewers.

Whole mount staining

Ear whole mounts were performed as previously described (Nitschke *et al.*, 2012). Briefly, ears were fixed in 1% PFA, split into two halves, blocked (12% bovine serum albumin), incubated with primary antibody, and were visualized with secondary antibodies. Z-stack confocal images were

obtained using a Leica SP5-U confocal microscope (Leica Microsystems Inc, Buffalo Grove, IL). Images were acquired using Zeiss Zen 2010 software (Carl Zeiss, Jena, Germany) and analyzed using Imaris version 7.2.3 software (Bitplane, Zurich, Switzerland).

Flow Cytometry

Flow cytometric analysis was performed on control and obese ear skin to characterize cell populations at baseline and post-challenge with DNFB as previously described (Zampell *et al.*, 2012). Briefly, single cell suspensions were prepared from ear skin by digesting tissues in a mixture of collagenase D, dispase and DNaseI for 45 minutes (Roche, Nutley, NJ). The cell suspension was then passed through a 70-micron filter. All filtered single cell suspensions were re-suspended in a 2% FCS solution. Cells were then incubated in CD16/CD32 (eBiosciences, San Diego, CA) to block endogenous Fc receptors and analyzed using a Fortessa multi-color flow cytometer (BD, San Jose, CA) with BD FACSDiva and FlowJo software (Tree Star, Ashland, OR). Cell populations were analyzed and defined using the cell surface markers CD45, CD3, CD4, CD8, CD25, CD69, F4/80, and CD11b (all BioLegend, San Diego, CA) using 3-5 animals/group/experiment.

Statistical analysis

Statistical analysis was performed using GraphPad Prism software (GraphPad Software, Inc., San Diego, CA). The Student's T-test was used to compare differences between two groups. Descriptive analysis and graphical methods were used to analyze and summarize results. Data is presented as mean ± standard deviation unless otherwise noted, with $p<0.05$ considered significant.

REFERENCES

Avraham T, Daluvoy S, Zampell J*, et al.* (2010) Blockade of transforming growth factor-beta1 accelerates lymphatic regeneration during wound repair. *Am J Pathol* 177:3202-14.

Nitschke M, Aebischer D, Abadier M*, et al.* (2012) Differential requirement for ROCK in dendritic cell migration within lymphatic capillaries in steady-state and inflammation. *Blood* 120:2249-58.

Zampell JC, Yan A, Elhadad S*, et al.* (2012) CD4(+) cells regulate fibrosis and lymphangiogenesis in response to lymphatic fluid stasis. *PLoS One* 7:e49940.

Supplemental Movies

Movies S1-4. Obese mice have impaired lymphatic pumping capacity. Representative NIR imaging videos of control and obese mice tails (movies 1 and 2, respectively) and hind limbs (movies 3 and 4) at baseline (i.e. without DNFB challenge).

Supplemental Figures

Figure S1. Obese mice ears have increased infiltration of $CD3^+$ cells at baseline.

- **a.** Representative immunofluorescence staining for CD3 (red) and LYVE-1 (green) in ear skin cross-sections of control and obese mice prior to DNFB challenge. DAPI nuclear stain is shown in blue. Scale bar=100μm.
- **b.** Quantification of $CD3^+$cells/HPF in ear cross-sections of control and obese mice prior to DNFB challenge (3HPF/animal and 5-8 animals/group; *$p<0.01$)

Figure S2. Obese mice have impaired lymphatic clearance.

- **a.** IVIS measurement of fluorescent signal intensity of dextran (2,000 kDa) from serum of lean mice at different time points after peripheral injection. Peak intensity was observed at 30 minutes post-injection.
- **b.** Representative IVIS images (top) showing the fluorescence signal intensity of FITC dextran (2,000 kDa) from serum of control and obese mice 30 min after peripheral injection. Quantification (bottom) of fluorescence intensity in control mice compared to obese (n=6-10 animals/group; *$p<0.05$).

Figure S3. Obese mice have normal antibody production but impaired T cell recall at baseline.

a. Quantification of anti-OVA IgG_1 antibody titers in obese mice as compared to control mice (p=NS).

b. Quantification of IFNγ levels in conditioned media from *ex-vivo* OVA-stimulated splenic T cells harvested from control or lean mice and previously vaccinated with or without OVA (*p<0.01 for control mice; p=NS for obese mice).

c. Quantification of IL-4 levels in conditioned media from *ex-vivo* OVA-stimulated T cells harvested from control or lean mice vaccinated with or without OVA (*p<0.05 for control mice; p=NS for obese mice).

d. Quantification of IFNγ protein expression in conditioned media from *ex-vivo* DNBS-stimulated splenic T cells harvested from control or lean mice 5 days following DNFB sensitization (*p<0.05 for control mice; p=NS for obese mice).

Figure S4. Obese mice have increased ear thickness after DNFB challenge.

a. Quantification of ear thickness fold change from baseline in control and obese mice 3 or 8 days following DNFB challenge (*p<0.05).

Figure S5. Obese mice have increased inflammation in response to a non-specific irritant (croton oil).

a. Representative histological cross section of ear skin sections harvested from control and obese mice 18 hours after topical croton oil challenge. Note increased ear and epidermal thickness in obese mice. Scale bar=200μm.

b, c. Quantification of ear thickness (**b**) and weight (**c**) of control and obese mice 18 hours following topical croton oil challenge (n=5-10; *p<0.01 for both).

Figure S6. Obese mice have increased generalized inflammation and accumulation of T cells in response to non-specific irritants (croton oil).

a, b. Representative immunohistochemical localization (**a**) and quantification (**b**) of $CD45^+$ cells in ear sections harvested from control and obese mice 18 hours after croton oil challenge (n=6-8 each; *p<0.01). Scale bar=100μm.

c, d. Representative immunohistochemical localization (**c**) and quantification (**d**) of $CD3^+$ cells in ear sections harvested from control and obese mice 18 hours after croton oil challenge (n=6-8 each; *p<0.01). Scale bar=100μm.

e, f. Representative immunohistochemical localization (**e**) and quantification (**f**) of $LYVE^+$ vessels/HPF in ear sections harvested from control and obese mice 18 hours after croton oil challenge (n=3 HPF/animal and 5 animals/group; *p<0.05). Scale bar=100μm.

Figure S7. Injection of rhVEGF-C does not increase blood vessel or macrophage expression of VEGFR-3.

a, b, c. Representative low power and high power (dashed box shown in separate inset panels in each figure piece) immunofluorescence localization of CD31 (green), VEGFR-3 (red), and LYVE-1 (blue) in histologic ear cross sections harvested from control or obese mice at baseline (**a**). White arrows illustrate the lack of blood vessel expression of VEGFR-3 in control mice and down regulation of VEGFR-3 on lymphatic vessels in obese mice at baseline (**a**). DNFB challenged animals were treated with daily subcutaneous ear injections of PBS or rhVEGF-C for 7 days followed by DNFB challenge and then 3 additional days of PBS or rhVEGF-C injections.

White arrows illustrate increased blood vessel expression of VEGFR-3 in control and in obese mice 3 days after DNFB challenge in mice treated with daily subcutaneous ear PBS injections (**b**). White arrows demonstrate no change in blood vessels expression of VEGFR-3 in control and obese mice after injection with rhVEGF-C (**c**). Scale bar=100μm.

d. Quantification of blood vessel counts (($CD31^+$/LYVE-1^- cells)/HPF) in groups outlined above. Note increase in blood vessel counts in both control and obese mice after DNFB challenge but no further increase after rhVEGF-C treatment (n=5-10; p=NS for all).

e. Representative low and high power (dashed area show in inset figures at the bottom of each figure piece) localization of CD11b (green), VEGFR3 (red), and DAPI in ear cross sections harvested 3 days after challenge with DNFB (upper panel) and in mice either treated with daily subcutaneous PBS or rhVEGF-C injections for 7 days prior to DNFB and 3 days after challenge (lower panel). Note no difference in macrophage expression of VEGFR-3 after rhVEGF-C treatment in both groups compared to their respective controls. Scale bar=100μm.

Figure S8. Injection of rhVEGF-C decreases infiltration of $CD45^+$ cells in both lean and obese mice 3 days after DNFB challenge.

a, b. Representative immunohistochemical localization (**a**) and quantification (**b**) of $CD45^+$ cells in ear cross sections harvested from control or obese mice 3 days following DNFB challenge. Animals were either treated with daily subcutaneous ear injections of PBS (top panels) or rhVEGF-C (lower panels) for 7 days followed by DNFB challenge and then 3 additional days of PBS or rhVEGF-C injections. (n=3 HPF/animal and 6 animals/group; *$p<0.01$). Scale bar=100μm.

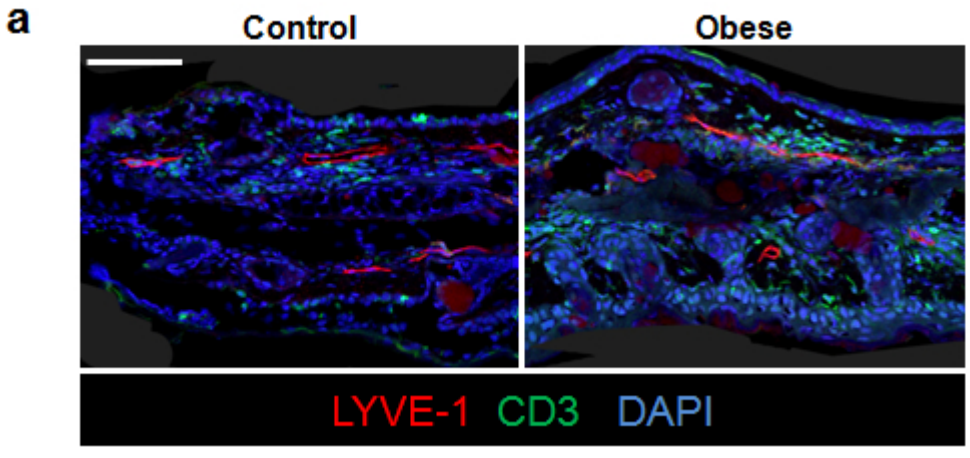
a
Control
Obese
LYVE-1 CD3 DAPI

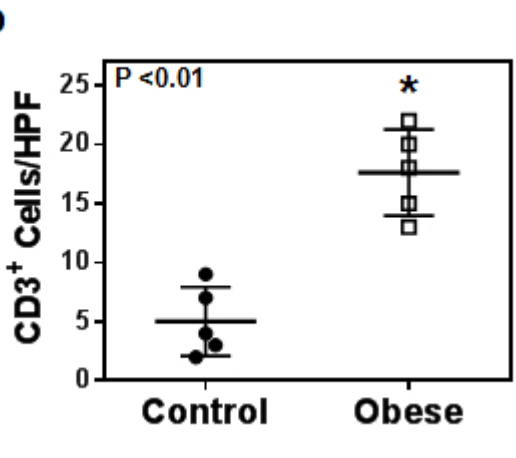
b
P <0.01
*
CD3+ Cells/HPF
25
20
15
10
5
0
Control
Obese

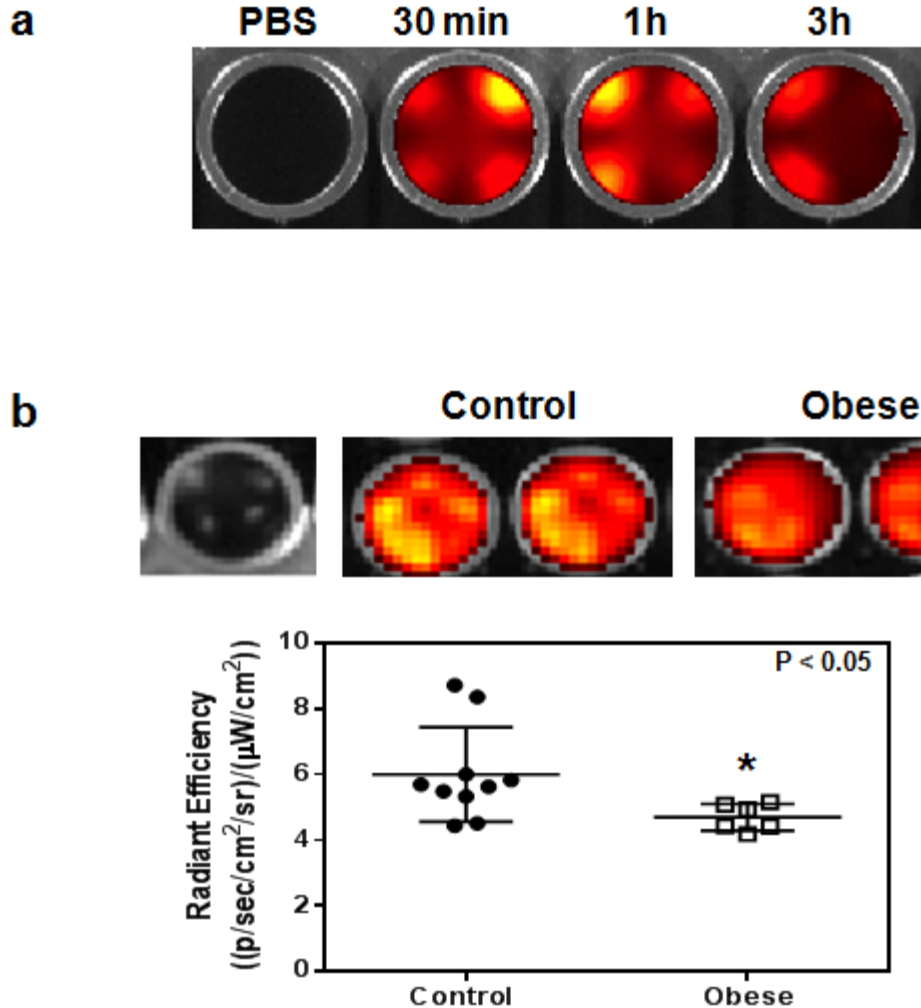
a
PBS
30 min
1h
3h
b
Control
Obese
Radiant Efficiency
((p/sec/cm2/sr)/(μW/cm2))
10
8
6
4
2
0
P < 0.05
*
Control
Obese

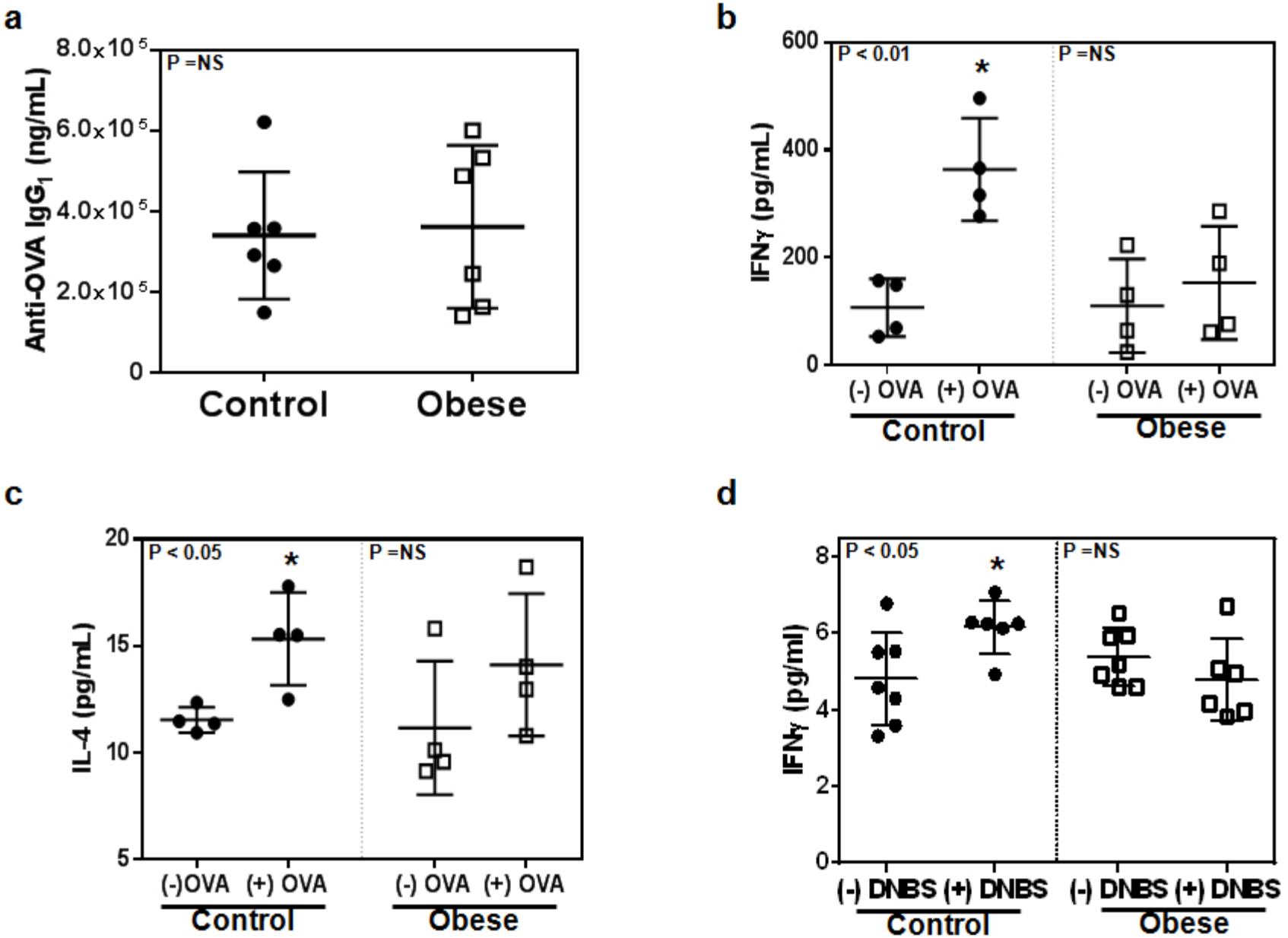
a
Anti-OVA IgG1 (ng/mL)
8.0x10^5
6.0x10^5
4.0x10^5
2.0x10^5
0
P =NS
Control
Obese
b
IFNγ (pg/mL)
600
400
200
0
P < 0.01
*
P =NS
(-) OVA
(+) OVA
(-) OVA
(+) OVA
Control
Obese
c
IL-4 (pg/mL)
20
15
10
5
P < 0.05
*
P =NS
(-)OVA
(+) OVA
(-) OVA
(+) OVA
Control
Obese
d
IFNγ (pg/ml)
8
6
4
2
0
P < 0.05
*
P =NS
(-) DNBS
(+) DNBS
(-) DNBS
(+) DNBS
Control
Obese

a

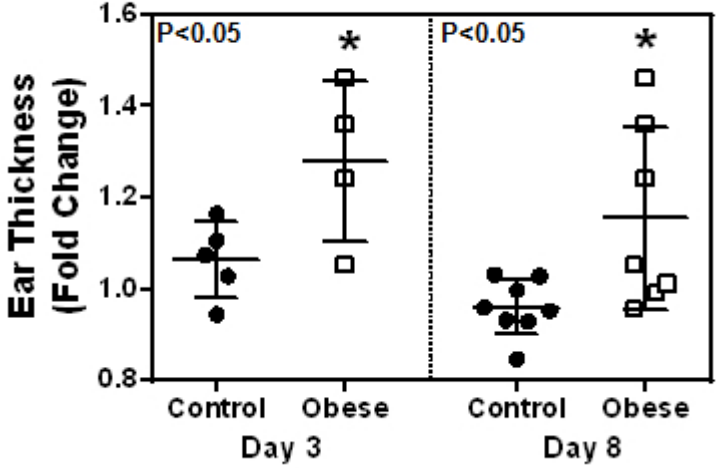
Ear Thickness
(Fold Change)
1.6
1.4
1.2
1.0
0.8
P<0.05
*
P<0.05
*
Control
Obese
Control
Obese
Day 3
Day 8

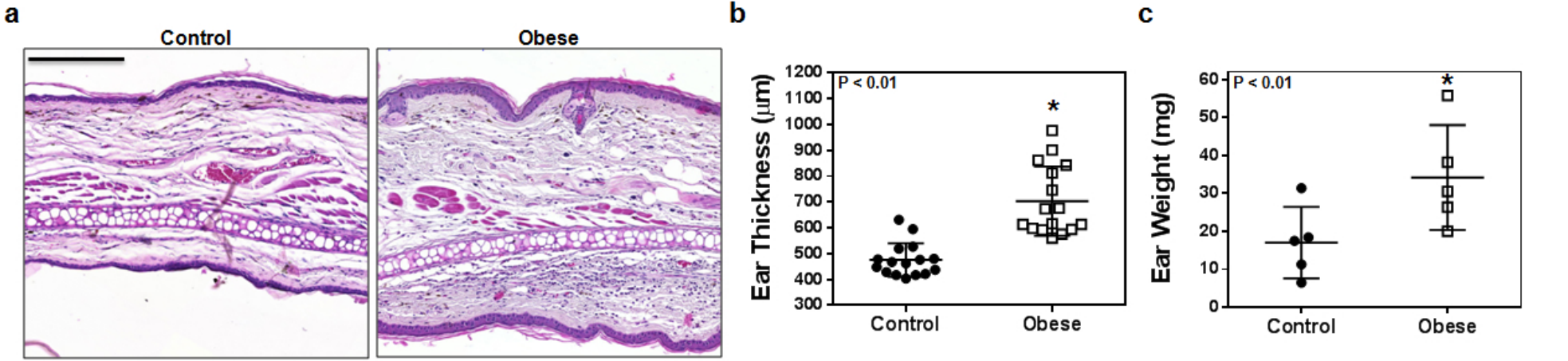
a
Control
Obese
b
Ear Thickness (μm)
P < 0.01
*
1200
1100
1000
900
800
700
600
500
400
300
Control
Obese
c
Ear Weight (mg)
P < 0.01
*
60
50
40
30
20
10
0
Control
Obese

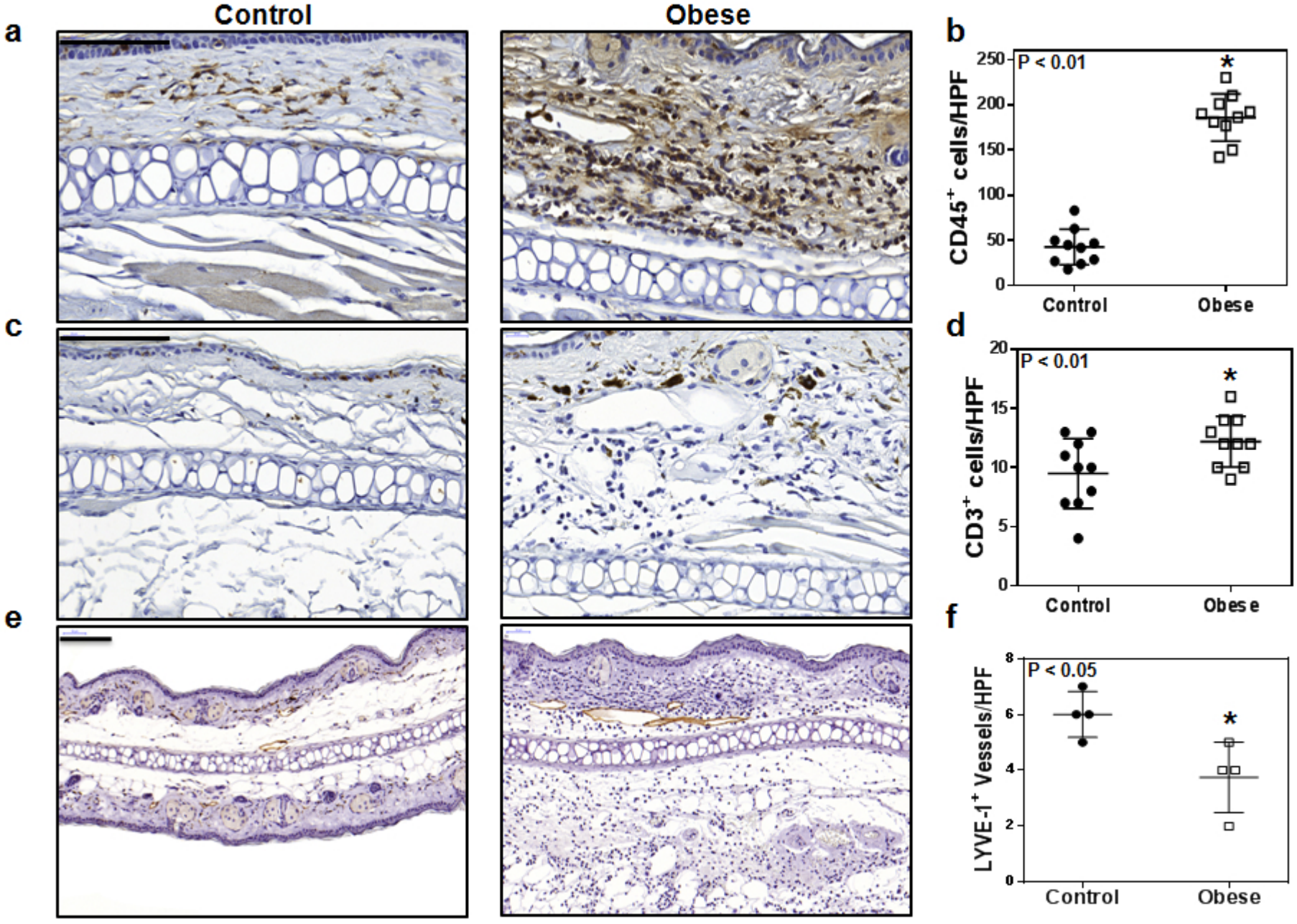
Control
Obese
a
b
c
d
e
f
P < 0.01
CD45+ cells/HPF
250
200
150
100
50
0
Control
Obese
*
P < 0.01
CD3+ cells/HPF
20
15
10
5
0
Control
Obese
*
P < 0.05
LYVE-1+ Vessels/HPF
8
6
4
2
0
Control
Obese
*

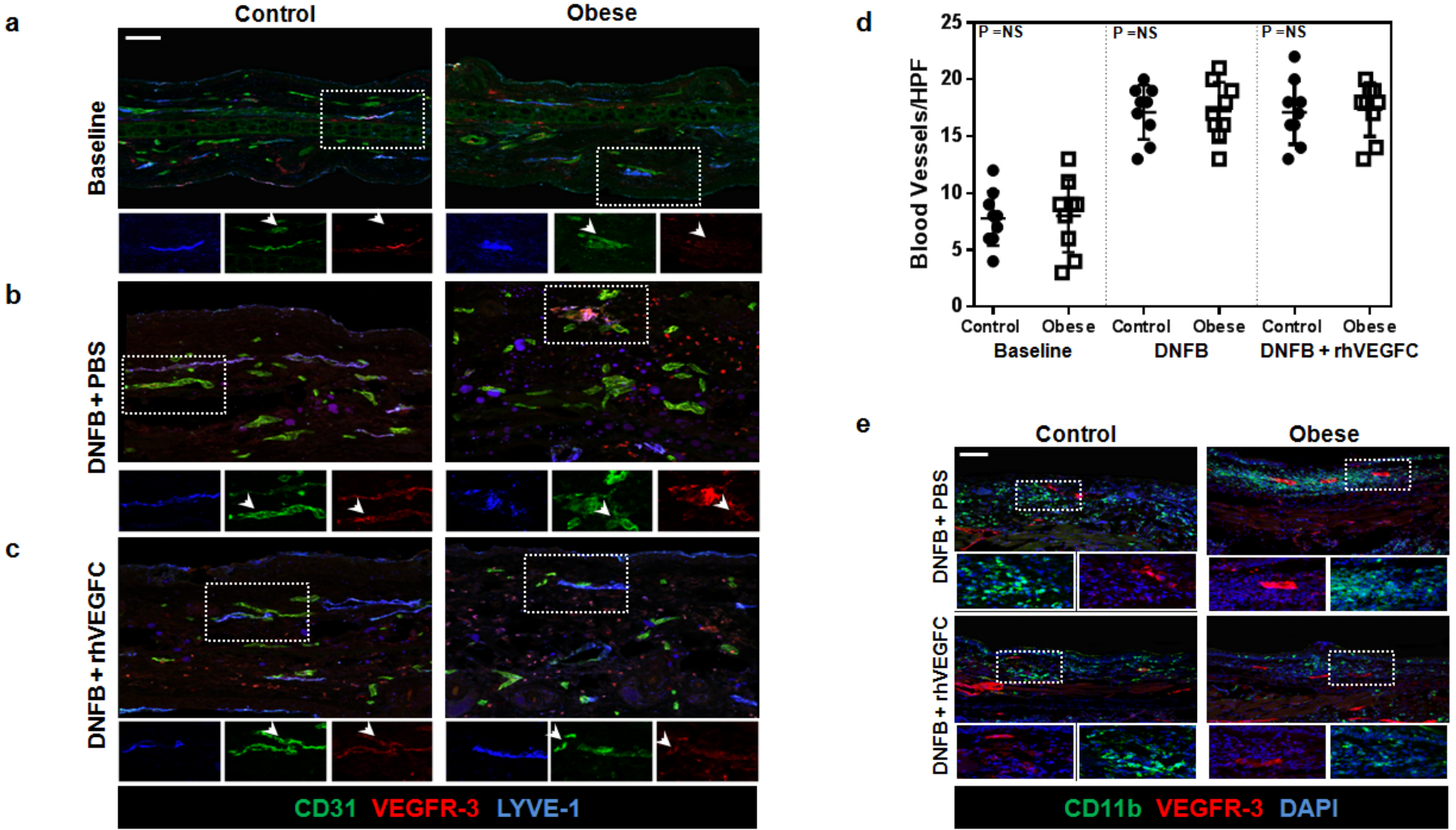
a
Control
Obese
Baseline
b
DNFB + PBS
c
DNFB + rhVEGFC
CD31 VEGFR-3 LYVE-1
d
Blood Vessels/HPF
25
20
15
10
5
0
P =NS
P =NS
P =NS
Control
Obese
Control
Obese
Control
Obese
Baseline
DNFB
DNFB + rhVEGFC
e
Control
Obese
DNFB + PBS
DNFB + rhVEGFC
CD11b VEGFR-3 DAPI

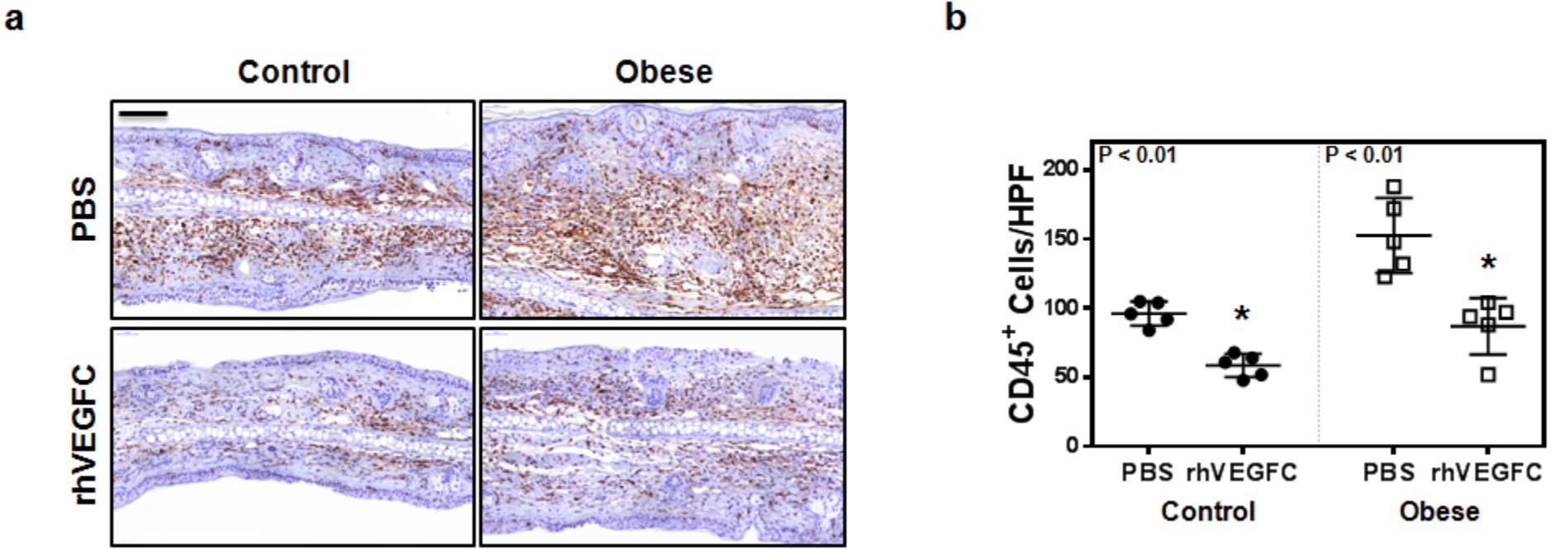
a
Control
Obese
PBS
rhVEGFC
b
P < 0.01
P < 0.01
CD45+ Cells/HPF
200
150
100
50
0
*
*
PBS
rhVEGFC
PBS
rhVEGFC
Control
Obese